Length Influences on Lateral Performance of Barrette from Three-Dimensional Finite Element Analysis

Der-Wen Chang[1*], Da-Wei Huang[1], Yung Kuang Lin[2], Fang-Chih Lu[2], Chin-Jung Kuo[2], and Askar Zhussupbekov[3]

[1] *Department of Civil Engineering, Tamkang University, 151 YinChuan Road, Tamsui District, New Taipei City, Taiwan 251*
[2] *Ground Master Construction Co., Ltd., & MICE Engineering Consultants, 1F, No.11, Lane 295, Sec. 1, Dunhua S. Rd., Da'an Dist., Taipei, Taiwan 106*
[3] *Department of Geotechnical Engineering, L.N. Gumilyov Eurasian National University, Munaitpassov street, Nur-Sultan, Kazakhstan, 010008*
[*] *Corresponding author. E-mail: dwchang@mail.tku.edu.tw*

Received: March 01, 2021; Accepted: October 1, 2021

The performance of a single barrette subjected to lateral load applied at its top is presented in this paper using three-dimensional finite element analyses based on Midas GTS program. Nonlinear behaviors of the barrettes buried in clayey and sandy soils were monitored using Mohr-Coulomb soil model. Performances of the barrettes with lateral loads applied in both longitudinal and transverse directions were examined. Displacements of the barrettes affected by stiffness and strength of the soils were obtained and normalized with the nominal length of the barrette. The criteria for long and rigid barrettes with loads in different directions were suggested. For the barrettes with loads in the transverse direction, the conventional analytical solution suggested by Chang for a single pile was found applicable to the predictions. In such case, the equivalent diameter calculated from moment of inertia of the barrette was found more adequate to be used in the analytical solution. Results of this study can help the engineers to understand more about the barrette performance under lateral loads.

Keywords: Barrette, Finite element analysis, Lateral performance, Horizontal load, Flexibility, Chang's formulas

http://dx.doi.org/10.6180/jase.202208_25(4).0003

1. Introduction

Barrette (or Barrette pile) has been used as one of the deep foundation structures in geotechnical engineering for decades [1–6]. In comparison with the single piles, the barrettes are known for higher resistances to sustain the loads applied in either vertical or horizontal directions.

The use of barrettes has been considered as an eco-solution that can provide economic benefits to foundation design. The performance of the barrette, including both capacity and serviceability, has been studied extensively in the past decades. Load capacities and deformations of the barrettes have been monitored by a number of studies [7–15]. It was learned that the conventional design for piles need special attentions to the barrettes. The behavior of barrette subjected to lateral loads is particularly of interest since the barrettes will be affected significantly by surrounding soils and load directions.

For lateral performance of the barrette, it has been pointed out that the load direction is an important factor [16]. It was indicated that if the load was applied at the longitudinal direction (i.e., x-axis) or at the transverse direction (i.e., y-axis) of the barrette, the barrette will respond differently. The load capacity and mobilized deformations of the barrette will be significantly increased if the load was applied in the longitudinal direction. For good lateral performance of the barrette, the designer must take into account the load direction.

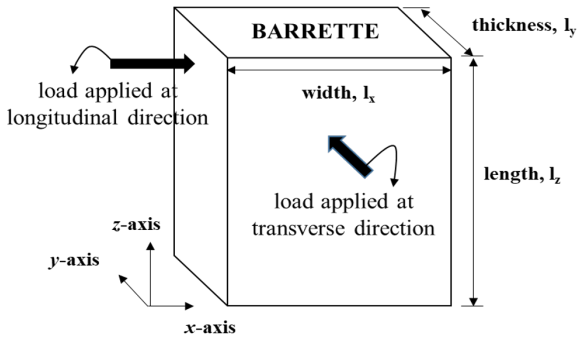

Fig. 1. Layout of the barrette and its dimensional parameters

Using the physical model of the barrettes in sandy soils, it has been shown that the increase of relatively density of sands will help to increase the lateral load capacity of barrette [17]. The effects of relative density of sands will decrease when the load was applied in the longitudinal direction of the barrette.

The ultimate capacity of a barrette loaded in transverse direction, whose cross-section ratio is around 2 3, would be approximately 40% of its ultimate capacity yielded by the same load in longitudinal direction. Fig. 1 reveals the longitudinal and transverse directions of a barrette and its dimensional parameters l_x, l_y and l_z defined in this study.

The numerical study on a concrete barrette (with cross section $l_x \times l_y$=2.8m $\times$ 1.2m) using FLAC3D analysis can be found in [18]. Nonlinear behaviors of the concrete barrette were monitored using Mohr-Coulomb soil model. It was reported that horizontal load of 2.2MN will make the barrette to crack.

When the load reached 5MN, the barrette will be yielded. Using the PLAXIS 3D analysis, it has been recently shown that the Mohr-Coulomb model and the hardening soil model can provide similar nonlinear results on the load-displacement curve of the barrette [19]. Again the load resistance of the barrette in the x-axis is much higher than that in the y-axis. In this study, the lateral performance of the barrette is examined again by three-dimensional Finite Element (FE) analysis.

The lateral behaviors of a concrete barrette embedded in homogeneous soil grounds of clays or sands are presented. The study intends to investigate the effects of barrette length combined with the load direction on deformations and internal stresses of the barrette.

2. 3D FE Analysis

Three-dimensional (3D) FE modelling has been known as the most rigorous computer-based method in the analysis of piled raft foundation [20]. It was popularly used in geotechnical engineering practice in the past decades.

The complexities and continuity of the structural geometry as well as the macroscopic material behaviors can be captured by 3D FE analysis. In simulating the barrette behaviors under vertically static loads, the authors [15] has pointed out that the 3D FE solutions and the 1D APILE analysis [20] can be different owing to discrete nature of the analysis. The simplified 1D analysis generally provides more conservative predictions rather than the 3D FE analysis. The FE analysis however would give more realistic results providing that the material parameters were calibrated adequately.

The FE analysis conducted in this study was made by Midas GTS NX package [21]. The Midas analysis has been used in many civil engineering projects in the past years. It can provide agreeable solutions with other well-known FE packages such as PLAXIS and ABAQUS. Essential boundaries (e.g., rollers and hinges) were generally used to model the FE boundaries. Fig. 2 depicts the boundaries used in the FE modeling.

Linear 8-node solid elements were used to discretize the zone of soils whereas a single barrette was located at its center. Verifications of the solutions were conducted by changing the length (L_x) and width (L_y) as well as the thickness (L_z) of the FE zone. The analyses in this study had been verified to yield stable solutions without influences of the boundaries and the discrete mesh (see Fig. 3). Fig. 4 depicts the comparison of Midas analysis [22] with those from ABAQUS analysis [23] using the Mohr-Coulomb soil model.

3. Numerical Model and Material Parameters

In this study, the width (l_x) and thickness (l_y) of the barrette were kept as 2.8m $\times$ 1.2m. The length (l_z) of the barrette was assumed at 50m and 20m, respectively. Young's modulus (E_c) and ν_c Poisson's ratio of the concrete barrette were assumed to be 3.5×10^4 MPa and 0.13. With the concern that the foundation structure should perform within the elastic range, the barrette was assumed linearly elastic.

Nonlinearities of the barrette were limited to the soils only. 8-node solid elements were used to model the barrette. A 4.5MN horizontal load was applied to the lateral side of the barrette at 1m height from the ground surface. The effects of applying either uniform load or concentrated load were examined, results indicated that the load-displacement curve of the barrette will be the same as long as the total load magnitude was the same.

The clayey and sandy soil profiles considered in this study are assumed homogeneous. Shear wave velocity

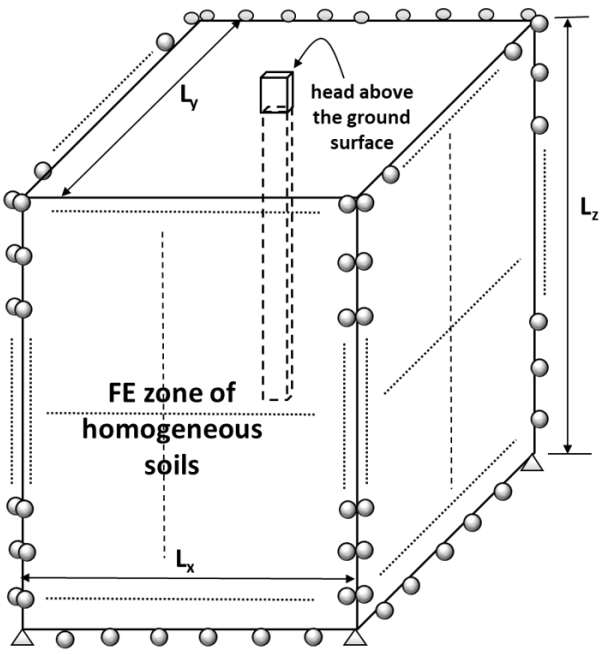

Fig. 2. Geometry and boundaries of FE analysis in this study

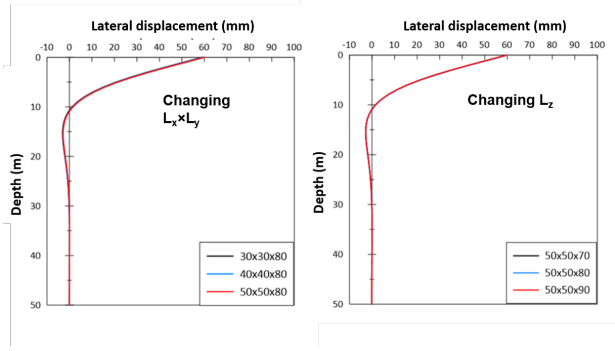

Fig. 3. Verification on solutions of the FE analysis with the size of analytical zone

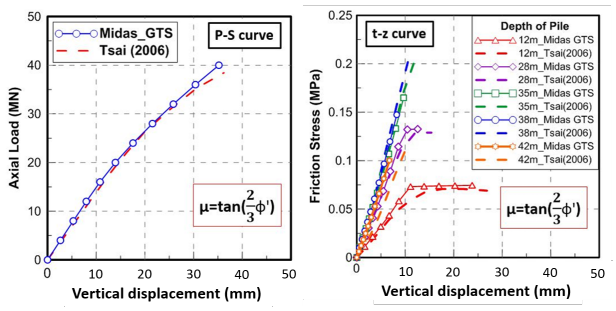

Fig. 4. Comparison of solutions from Midas analysis and ABAQUS analysis (from [23])

(V_s) of the soils was assumed at 120, 150 and 180m/s to simulate the soft soil sites (Type-III ground) specified in seismic design code in Taiwan [24]. For clays, the soils were assumed having the Poisson's ratio (μ) of 0.4 and unit weight (γ_s) of 20kN/m^3.

The corresponding Young's modulus (E_s) of the soil can be calculated by $2 \times V_s^2 \rho_s (1+\mu)$, where ρ is mass density ($=\gamma_s/g$) of the soil and g is the acceleration of gravity. Since the Mohr-Coulomb model was used, empirical equation [25, 26] as shown in Eq. (1) was used to compute the undrained shear strength (S_u) of the clays. The corresponding undrained shear strength (S_u) of the clays was computed as 32, 52 and 76kPa, respectively.

$$V_s = 23 s_u^{0.475} \ (V_s \text{ in m/s}; S_u \text{ in kPa}) \tag{1}$$

For sands, the Poisson's ratio of 0.3 and unit weight of 19kN/m^3 was assumed. The empirical formula expressed in Eq. (2) [24] was used to compute the corresponding SPT-N values. With the SPT-N values obtained, the empirical formulas for medium dense sand shown in Eq. (3) [27] was used to obtain the friction angle (ϕ) of the sands. Corresponding drained friction angles of the sands were obtained as 28°, 31°, 34°, respectively. Table 1 summarizes the structural geometry and material parameters used in the study.

$$V_s = 80 \times (N)^{0.33} \ (V_s \text{ in m/s}) \tag{2}$$

$$\phi = 3.5 \times (N)^{0.5} + 21 \text{ (degrees)} \tag{3}$$

In order to interpret the barrette displacements affected by the relative stiffness between the barrette and the soils, the nominal lengths of a single pile in clays [28] and those in sands [29] were adopted. For clayey soils, the nominal length (R) of the barrette (treated as a pile) can be calculated using Eq. (4).

$$\mathrm{R} = \sqrt[4]{\frac{E_c I_c}{k}} \tag{4}$$

Where Ic is the moment of inertia of the pile, k is the relative stiffness between pile and soil (units in F/L^2) which can be denoted by Eq. (5),

$$k = 0.65 \sqrt[12]{\frac{E_s \mathrm{D}_e^4}{E_c I_c}} \frac{E_s}{1-\mu^2} \tag{5}$$

In above equation, D_e is the equivalent diameter of the barrette. For a pile with length L, it was suggested that when $\mathrm{L/R} \geq 5$, the pile is long pile. If $\mathrm{L/R} \leq 2$, the pile became rigid pile [28]. Because the load can be applied at the transverse direction (y-axis) and the longitudinal direction (x-axis), the corresponding moment of inertia of the

Table 1. Structural geometries and material parameters of the numerical model

Structural geometries	**Barrette**: $L_x \times L_y \times L_z$=2.8m × 1.2m × 50m(or 20m) **Zone of the soils**: $L_x \times L_y \times L_z$=50m × 50m × 80m
Material parameters	Concrete barrette: E_c=35000 MPa;ν_c =0.13; γ_c=24kN/m^3 Clayey soils: V_s=120, 150, 180m/s; μ=0.4; γ_s=20kN/m^3 E_s=82, 128, 185 MPa; $S_u \cong$ 32, 52, 76 kPa Sandy soils: V_s=120, 150, 180m/s; μ=0.3; γ_s=19kN/m^3 E_s=73, 113, 163 MPa; $\phi \cong 28^\circ, 31^\circ, 34^\circ$

Table 2. Nominal length of the barrette used in this study

V_x	Clay		Sand	
(m/s)	R_x (m)	R_x (m)	T_x (m)	T_y (m)
120	4.04	6.41	5.11	7.19
150	3.58	5.68	4.72	6.63
180	3.24	5.14	4.45	6.26

barrette are expressed by I_{cx} and I_{cy}, respectively. Therefore, for load applied in transverse direction, the nominal length is termed as R_x. In contrast, the nominal length is termed as R_y for load applied in the longitudinal direction.

For sandy soils, the nominal length T was calculated using Eq. (6). The long pile and rigid pile criteria were suggested similarly as those for the clays, i.e., L/T $\geq$ 5 for long piles and L/T $\leq$ 2 for rigid piles [29].

$$\mathrm{T} = \sqrt[5]{\frac{E_c I_c}{n_h}} \tag{6}$$

In above equation, n_h is the coefficient of subgrade reaction (units in F/L^3). The correlation suggested by [30] was adopted to estimate the subgrade reaction coefficients (n_h) for sands. The coefficient of subgrade reaction, nh was approximated by knowing the shear wave velocities of the soils.

The resulted n_h was computed as 4000, 6000 and 8000kN/m^3. Again, T_x and T_y can be found for loads applied in different directions. Table 2 reveals the nominal lengths of the barrette used in this study with the dependence of clays and sands varying the shear wave velocities and loads in different directions.

4. Lateral Performance of Barrette

The barrette model was subjected to a horizontal load of 4.5MN. To obtain nonlinear behaviors of the barrette, the load was divided into 40 steps with the load increment of 112.5kN. The convergences of the solutions were ensured to yield the barrette displacements.

The lateral load was applied in the transverse direction and the longitudinal direction aside the barrette. Load-displacement curves of the barrette at where the load was applied, and the lateral displacements, internal bending moments and shear forces along the barrette were monitored. The moments and shears along the barrette were further computed with the displacements and rigidity term EI from the analytical equations.

4.1. Load in transverse direction

4.1.1. Barrette in clays

Fig. 5 presents the behaviors of a 50m barrette in clays, which comprises the load-displacement curve recorded at the ground surface, and displacements, moments and shears along the barrette subjected to lateral load in the transverse direction. Fig. 6 shows similar behaviors of a barrette with 20m length.

Since the displacements at the bottom of the barrette were not vanished, the last two meters of the barrette was presumed to compute the bending moment and shear at 20m. The effects of soil stiffness in terms of the shear wave velocity of the soil are clearly revealed in Figs. 5 and 6. It can be found that maximum displacements of the barrette are in similar scale (40∼100mm) regardless of the length of barrette. Shorter barrette was more rigid while longer barrette showed more flexural deflections.

The displacements will decrease with the increase of soil stiffness. The influences of soil stiffness are more significant to the bending moments compared to the shear forces. For the shorter barrette, moments and shears were found along the whole barrette. For longer barrette, the moments and shears will vanish below the length at 0.5L (where L=l_z).

4.1.2. Barrette in sands

Fig. 7 presents the behaviors of the 50m barrette in sands under horizontal load applied in the transverse direction. Fig. 8 shows the behaviors of the barrette with length of 20m. It can be found that the soil stiffness become less significant compared to those found in clays.

Similar displacements were found in the maximum rages of 80∼130mm for both long and short barrettes. Shorter barrettes will deform without showing the inflection point. Again, the influences of the soil stiffness are relatively insignificant to the shear forces in comparison with the bending moments. Again for the longer barrette,

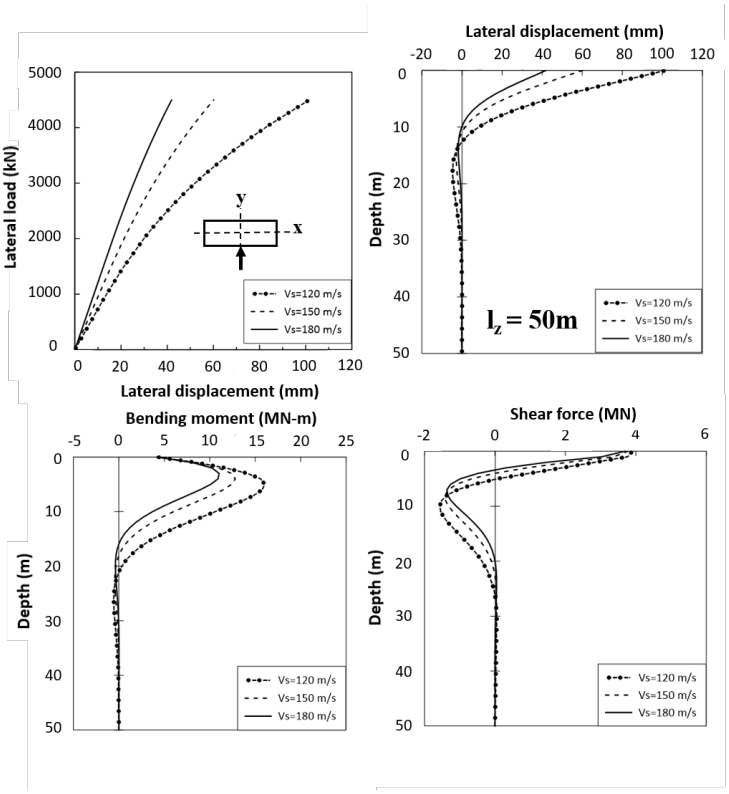

Fig. 5. Performance of 50m barrette in clays with load applied in transverse direction

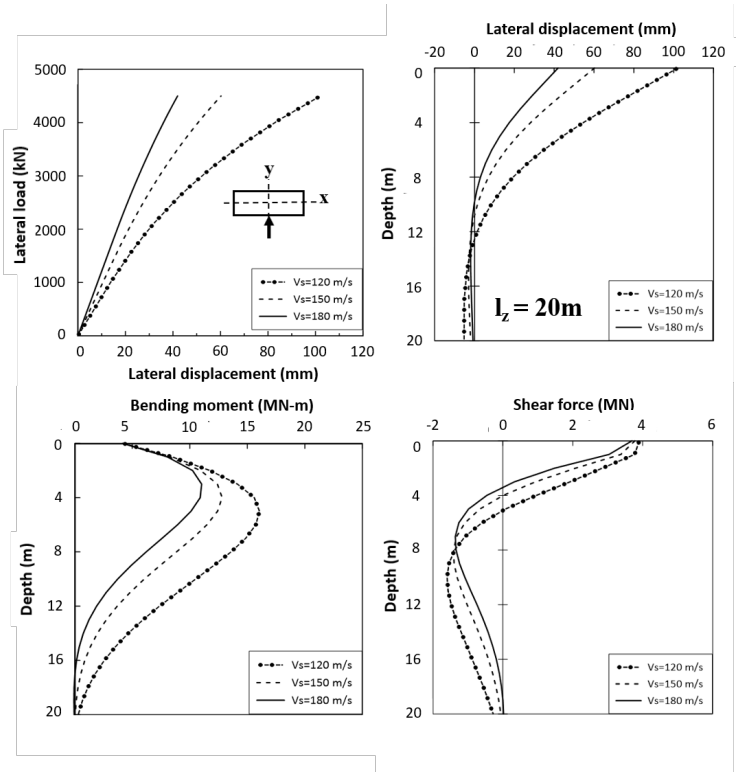

Fig. 6. Performance of 20m barrette in clays with load applied in transverse direction

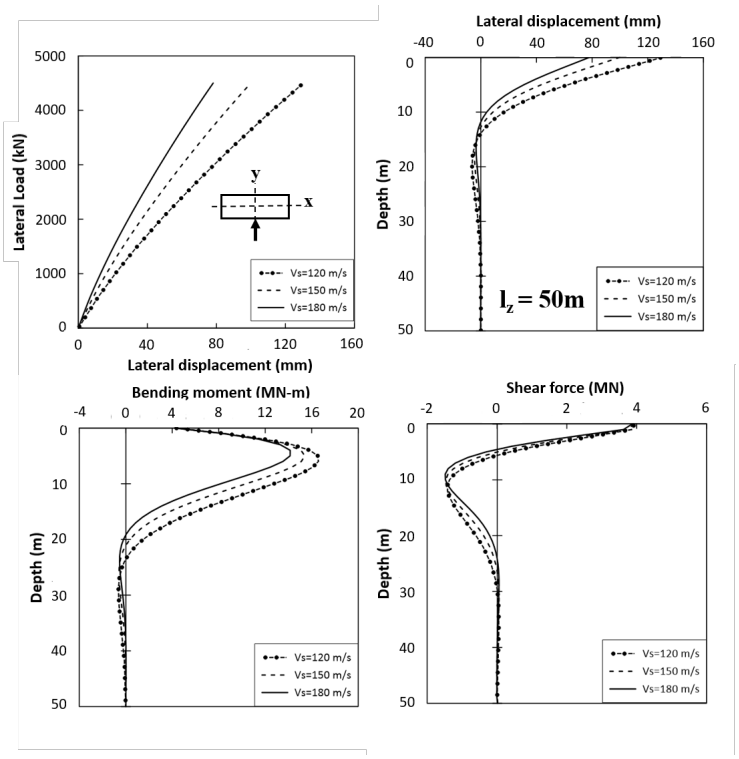

Fig. 7. Performance of 50m barrette in sand with load applied in transverse direction

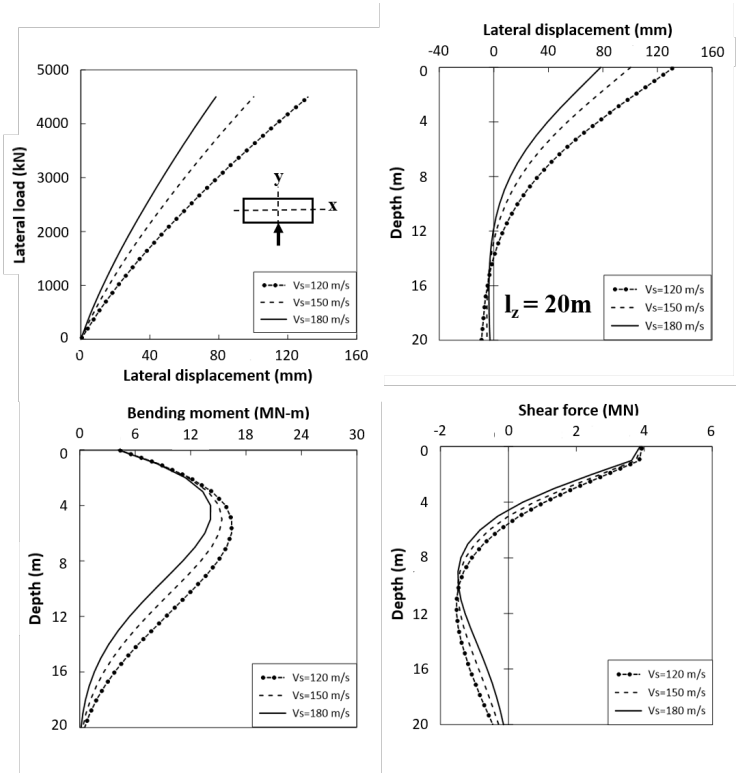

Fig. 8. Performance of 20m barrette in sands with load applied in transverse direction

most of the deflections, moments and shears were found within the length of 0.5L of the barrette.

4.2. Load in longitudinal direction

4.2.1. *Barrette in clays*

For load in longitudinal direction, Fig. 9 and Fig. 10 depict the behaviors of the barrettes in clays with its length at 50m and 20m respectively. Now the effects of soil stiffness are becoming smaller.

The maximum displacements (30∼ 60mm) of the barrette are smaller than those caused by the loads in transverse direction. Comparing with those found in Figs. 5 and 6 , the increase of structural stiffness will affect the performance of barrette significantly. For load applied in longitudinal direction of the longer barrette, the influences of the displacements, moments and shears were then appearing in 0.8L of the barrette.

4.2.2. *Barrette in sands*

Fig. 11 and Fig. 12 show the corresponding behaviors of the barrettes in sands with 50m and 20m length. The maximum displacements in this case became 60∼125mm for the shorter barrettes and 50∼90mm for the longer barrettes.

The longer barrette in sands can provide much greater resistance than the shorted barrette if the load was applied at the longitudinal directions. The observation on displacements, moments and shears along the length of 0.8L of the barrette was again clearly shown for the longer barrette in sands.

5. Flexibility of Barrette

The criteria to determine long barrette and rigid barrette are helpful to design engineers. A rigid short barrette would react similarly as a rigid underground wall against the lateral loadings. A long barrette would behave more like a flexible underground structure against the lateral loads.

Following discussions were made for barrettes in clays and sands. Knowing that u and v are the corresponding displacements of the barrette in x- and y- directions, the normalized displacements v/R_x and v/T_x were monitored for loads in transverse direction, and u/R_y and u/T_y were used for loads in longitudinal direction.

5.1. Barrette in clays

Varying the shear wave velocities of the soils (V_s) at 120, 150 and 180m/s of the clays, and mounting the horizontal loads of 4.5MN in the transverse or the longitudinal directions onto the barrette, the normalized displacements can be shown in Figs. 13 to 15. Table 3 depicts the corresponding values of the ratios of L/Rx and L/Ry.

From the plots, one can conclude that $L/R_x \geq 5$ can be used as the criterion of long barrette when the load is applied in transverse direction. It was found that for the barrettes with length of 20 ∼ 50m in clays and where the load is in transverse direction, the barrettes will all react in flexible manner.

Thus the study did not reduce the length to yield rigid barrette. On the other hand if the load was applied in longitudinal direction, it was found that $L/R_y \geq 7$ can be used for criterion of long barrette, and $L/R_y \leq 3$ can be used to define rigid barrette.

5.2. Barrette in sands

Varying the shear wave velocities of the soils (V_s) at 120, 150 and 180m/s of the sands, and mounting the horizontal loads 4.5MN in the transverse or the longitudinal directions onto the barrette, Figs. 16 to 18 and Table 4 depict the corresponding results.

From the plots, one can conclude that $L/T_x \geq 6$ can be the criterion for long barrette when the load is applied in transverse direction, and when $L/T_x \leq 2$ it can be used for rigid barrette. When the load is applied in longitudinal direction, it can be also found that $L/T_x \geq 6$ and $L/T_x \leq 2$ are working well for long barrette and rigid barrette, respectively.

The above studies indicate that the barrette in clayey strata and in sandy strata can be very different. The designer needs to be aware of such performance when consider the barrette resistance in different directions.

6. Comparisons with Chang's Formulas

In order to learn the applicability of mathematic equations suggested by Chang [31] to the barrettes, the displacements, moments and shears along the barrette in clays and sands (where V_s=150m/s) were obtained from corresponding equations. Because the mathematic functions were proposed for the round pile, so the equivalent diameter (D_e) was calculated prior to the computations.

This study computed the values D_e from both the area (A) and the moment of inertia (I_c) respectively. For load applied in various directions, I_{cx} and I_{cy} need to be distinguished. The values of the equivalent diameter De with respect to the area A, Icx and Icy are obtained as 2.06m, 1.69m and 2.59m in this study.

Figs. 19 and 20 depict the comparisons of the barrette performances in clays when the loads were applied in transverse and longitudinal directions respectively. It can be found that the prediction from Chang's formulas using D_e from area of the cross section would provide smaller maximum displacements compared to the 3D FE solutions.

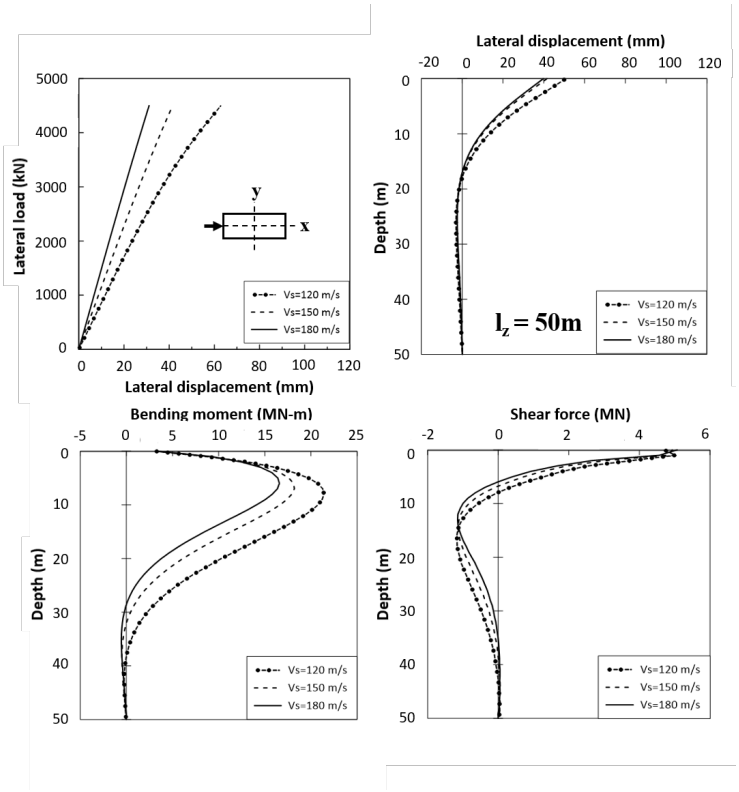

Fig. 9. Performance of 50m barrette in clays with load applied in longitudinal direction

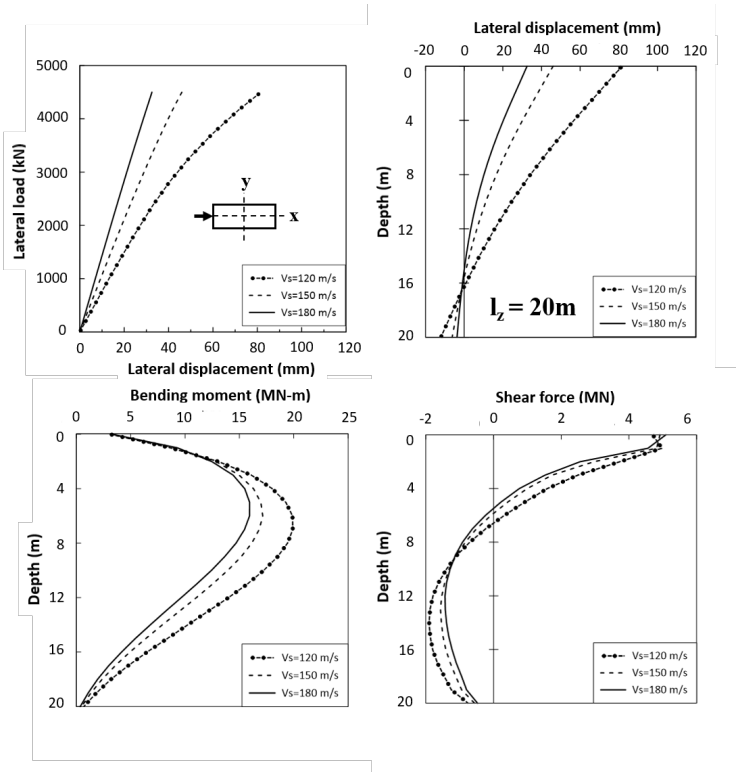

Fig. 10. Performance of 20m barrette in clays with load applied in longitudinal direction

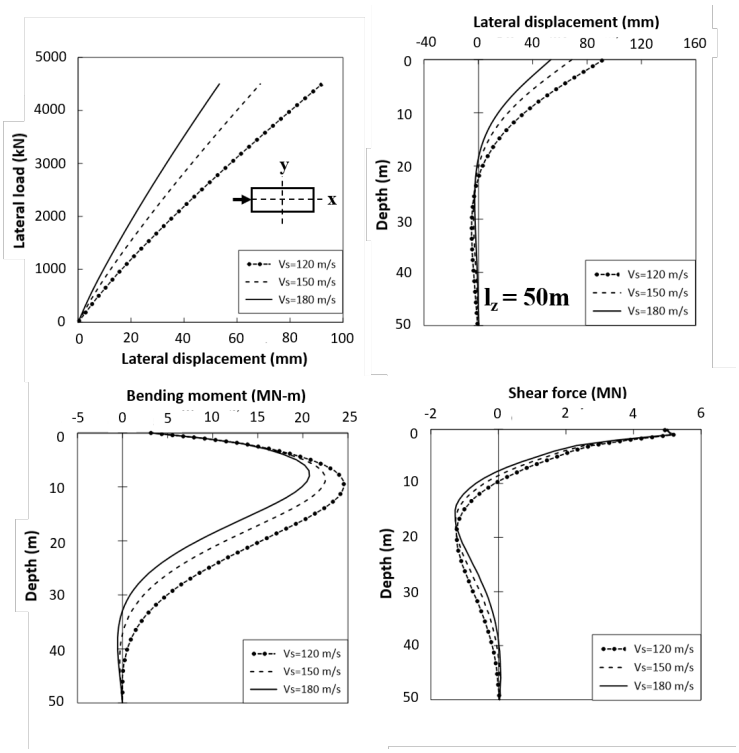

Fig. 11. Performance of 50m barrette in sands with load applied in longitudinal direction

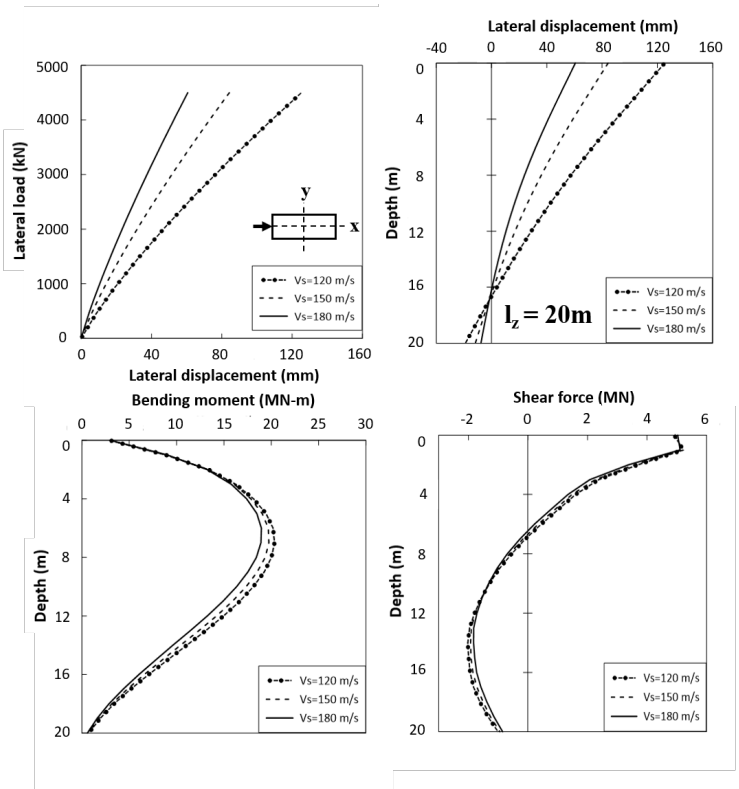

Fig. 12. Performance of 20m barrette in sands with load applied in longitudinal direction

Table 3. Normalized length of barrettes in assessing the flexibility of barrette in clays

V_s / L(m)	120m/s		150m/s		180m/s	
	L/R_x	L/R_y	L/R_x	L/R_y	L/R_x	L/R_y
20	4.95	3.12	5.59	3.52	6.17	3.89
30	7.43	4.68	8.37	5.28	9.26	5.84
40	9.9	6.24	11.17	7.58	12.35	7.78
50	12.38	7.8	13.97	8.8	15.43	9.73

Table 4. Normalized length of barrettes in assessing the flexibility of barrette in sands

V_s / L(m)	120m/s		150m/s		180m/s	
	L/T_x	L/T_y	L/T_x	L/T_y	L/T_x	L/T_y
10	1.96	1.39	2.12	1.51	2.24	1.59
15	2.94	2.09	3.18	2.26	3.37	2.4
20	3.91	2.78	4.24	3.02	4.49	3.19
25	4.59	3.47	5.3	3.77	5.62	3.99
40	7.83	5.56	8.47	6.03	8.98	6.39
50	9.78	6.95	10.6	7.54	11.23	7.99

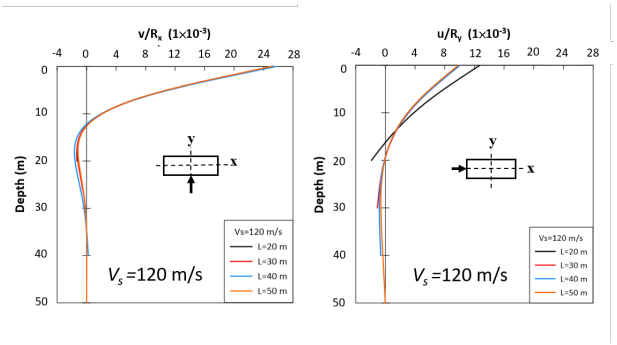

Fig. 13. Normalized deflections of the barrette in clays (v_s=120m/s)

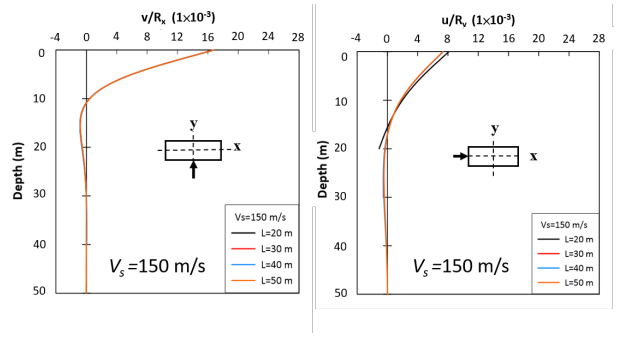

Fig. 14. Normalized deflections of the barrette in clays (v_s=150m/s)

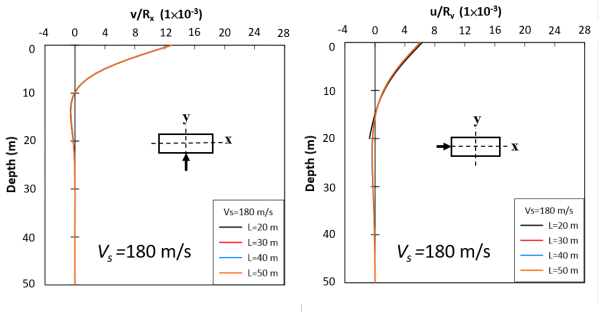

Fig. 15. Normalized deflections of the barrette in clays (v_s=180m/s)

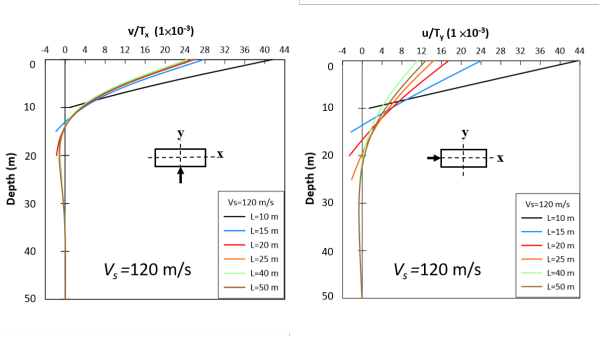

Fig. 16. Normalized deflections of the barrette in sands (v_s=120m/s)

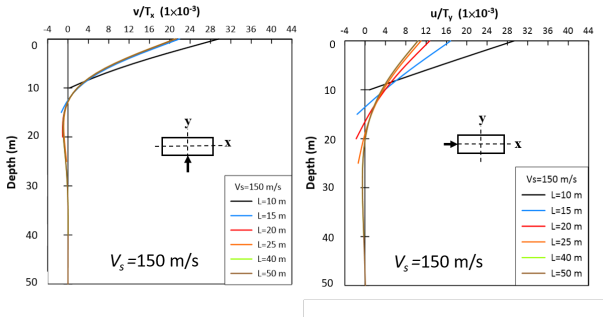

Fig. 17. Normalized deflections of the barrette in sands (v_S=150m/s)

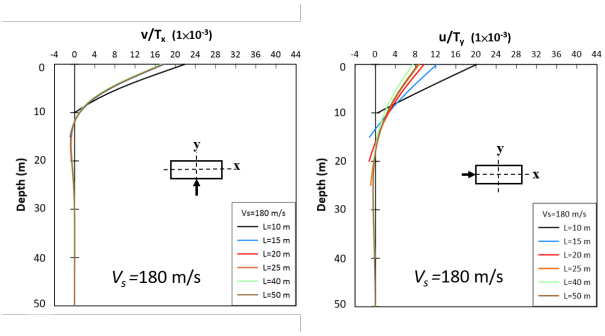

Fig. 18. Normalized deflections of the barrette in sands (v_S=180m/s)

Despite that the maximum displacements were found compatible for loads applied at different directions, the deflections along the barrette were found quite different from the analytical solutions.

The maximum bending moments and the shapes of moments along the barrette were found similar when the load was applied in the transverse direction. In such case, the maximum shear forces would be overestimated in shallow parts of the barrette.

If the load was applied in the longitudinal direction, the maximum bending moments from the analytical solutions will be significantly underestimated. The associated maximum shear forces along the barrette would be overestimated, and they seemed to remain at the depths between 0∼10m from the ground surface of the barrette.

Figs. 21 and 22 reveal the results for barrettes in sands. Similar observations can be found for barrette in sands. It can be concluded that the Chang's formulas for the piles are applicable to barrettes in sands when the load is applied to the transverse direction at the barrette with the equivalent diameter, D_e of the barrette obtained from the moment of inertia.

However, if the load is applied in the longitudinal direction of the barrette, the applications of the Chang's formulas will need special attentions since the bending moments of the barrette could be significantly underestimated.

7. Concluding Remarks

The performance of a single barrette subjected to lateral load above the ground surface was studied using three-dimensional finite element modeling of Midas package. The numerical model of barrette was assumed in clayey and sandy soils respectively. Mohr-Coulomb model of the soil was adopted for undrained clays and drained sands.

The horizontal load with a magnitude of 4.5MN was applied to the barrette at one-meter height above the ground surface, thus a bending moment of 4.5MN-m was resulted at the ground surface to the barrette. Loads were applied respectively in transverse and longitudinal directions to the barrettes with different length at 50m and 20m. Results of this study are summarized as follows.

1. For the numerical model of the barrette (2.8m × 1.2m), if the load is applied in the transverse direction, the 50m barrette will exert bending moments and shear forces up to a depth of 0.4L (i.e., 20m), where L stands for length of the barrette (=50m). Similar phenomenon was observed for barrettes in both clays and sands. However if the load was applied in longitudinal direction, the affected length of the moments and shears will increase to least 0.6L (i.e., 30m) of the longer barrette in clays and sands. The shorter barrettes were found to yield relatively larger maximum displacements than the longer barrette especially in the cases of sands.

   Such phenomenon is caused by the rigidity of the barrette and the relative stiffness between the barrette and the soils. The observation implies that the modelled barrettes at soft sites ($V_s \leq$ 180m/s should be least 30m long to resist the applied horizontal loads.

2. For barrettes installed in clays, if the load was applied in transverse direction, $L/R_x \geq 5$ can be used as the criterion for long barrette (no moment and shear at the bottom of barrette), where R_x is the nominal length of the barrette when moment of inertia computed across the x-axis. If the load was applied at longitudinal direction, it was found that $L/R_y \geq 7$ can be used for long barrette, and $L/R_y \leq 3$ can be used to determine the rigid barrette. Similarly, R_y is the nominal length of the barrette with respect to the y-axis.

3. If the barrette is installed in sands, it was found that $L/T \geq 6$ and $L/T \leq 2$ can be used to determine long

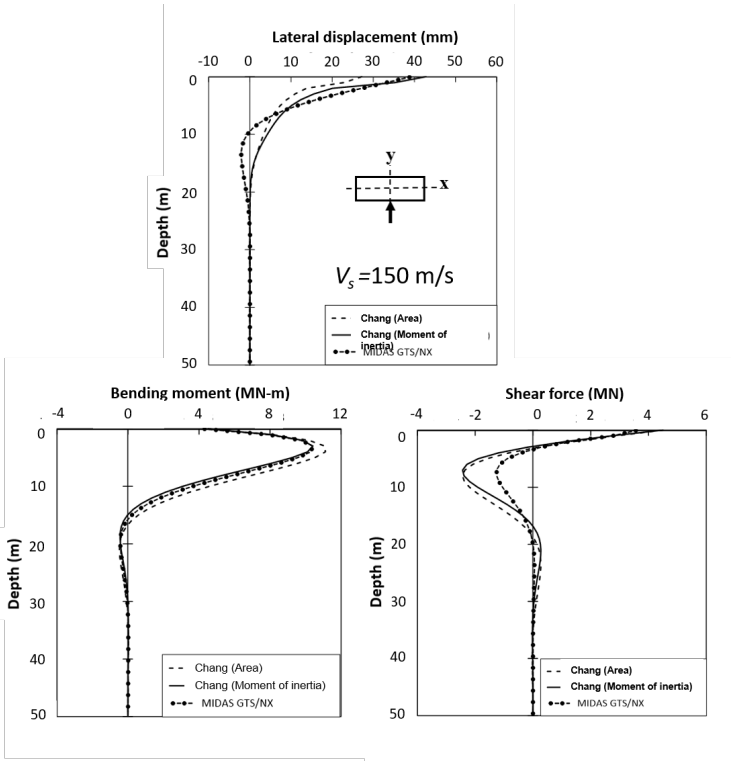

Fig. 19. Performance of barrette in clays with load applied in transverse direction

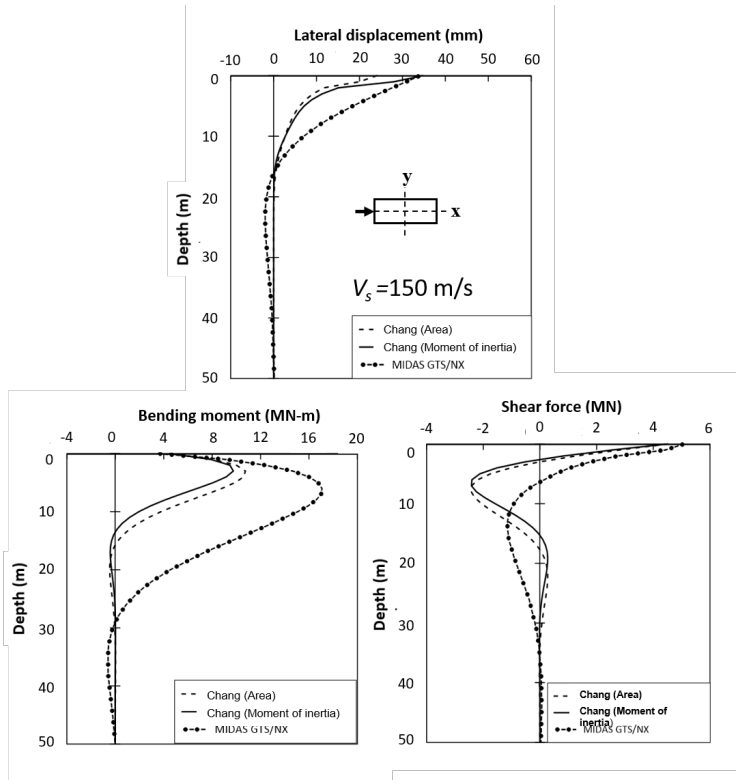

Fig. 20. Performance of barrette in clays with load applied in longitudinal direction

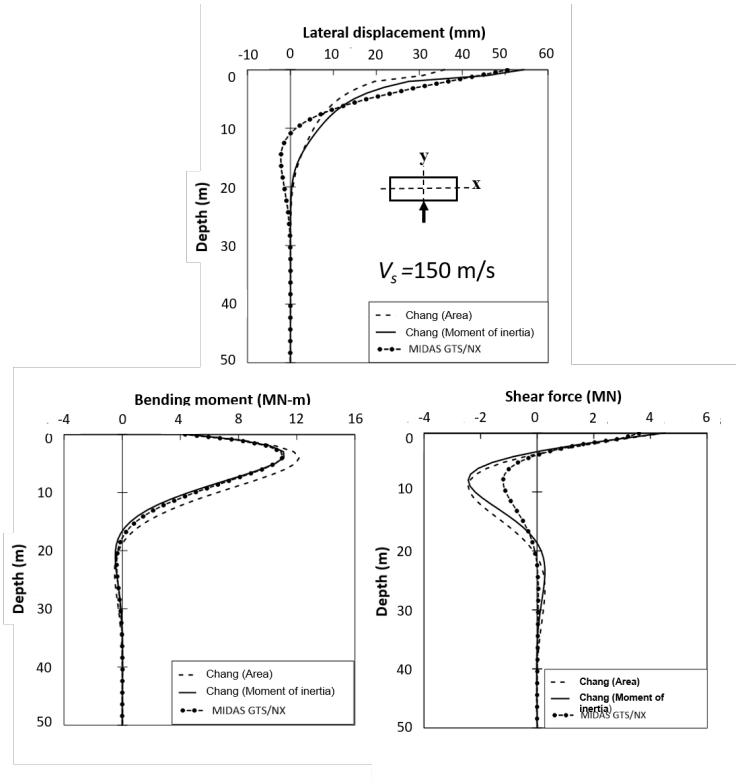

Fig. 21. Comparative solutions for barrette in sands with load in transverse direction

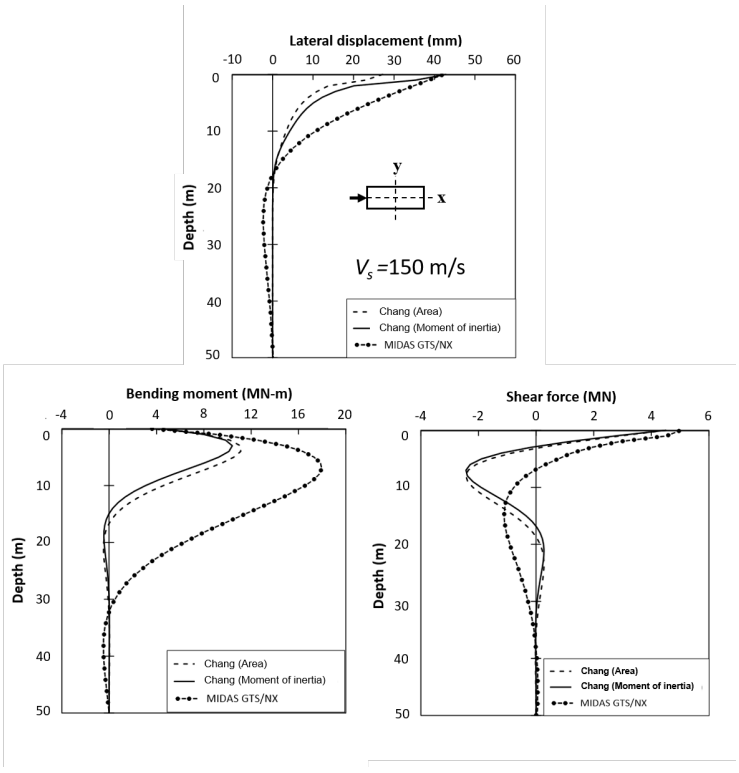

Fig. 22. Comparative solutions for barrette in sands with load in longitudinal direction

barrette and rigid barrette, respectively. The criteria are applicable regardless of the direction of load. The nominal length T needs to be computed accordingly with respect to the loading direction.

4. Analytical formulas suggested by Chang [31] on single piles subjected to lateral loads were found adequate for barrette in the cases where the load is applied in transverse direction and the equivalent pile diameter is obtained from the moment of inertia of the barrette. In any case if the load was applied in longitudinal direction, the bending moments along the barrette would be significantly underestimated using the analytical formulas.

5. Solid finite elements were adopted only in this study to simulate the barrette responses. The hybrid element model where both solid concrete elements and beam elements of steel bars are considered could receive further attentions for advanced research work.

6. The study was made assuming that the concrete barrette remains linearly elastic. For considerable horizontal loads which may cause the barrette to crack and damage further, the conclusions should be cautioned.

Acknowledgements

This study is supported by the research fund from Ground Master Construction Co., Ltd./MICE Engineering Consultants in Taiwan. Gratefulness of the authors also extended to Dr. Chin Der Ou, Mr. Chung-Cheng Kao and Prof. San-Shyan Lin for comments and suggestions in reviewing the results.

References

[1] S. D. Ramaswamy and E. Pertusier, (1986) *"Construction of barrettes for high-rise foundations"* **Journal of construction engineering and management *112***(4): 455–462. DOI: 10.1061/(ASCE)0733-9364(1986)112:4(455).

[2] K. Ho. *Behaviour of the Instrumented Trial Barrette for the Trademart Development at NKIL 6032, Kowloon Bay*. Geotechnical Engineering Office, Civil Engineering Department, 1994.

[3] C. Shen, C. W. W. Ng, W. Tang, and D. Rigby. "Testing a friction barrette in decomposed granite in Hong Kong". In: *Fourteenth International Conference on Soil Mechanics and Foundation Engineering. ProceedingsInternational Society for Soil Mechanics and Foundation Engineering*. **4**. 1999.

[4] B. H. Fellenius, A. Altaee, R. Kulesza, and J. Hayes, (1999) *"O-cell testing and FE analysis of 28-m-deep barrette in Manila, Philippines"* **Journal of Geotechnical and Geoenvironmental Engineering *125***(7): 566–575. DOI: 10.1061/(ASCE)1090-0241(1999)125:7(566).

[5] N. Thasnanipan, A. W. Maung, and G. Baskaran. "Diaphragm Wall And Barrette Construction For Thiam Ruam Mit Station Box, Mrt Chaloem Ratchamongkhon Line, Bangkok". In: *ISRM International Symposium*. OnePetro. 2000.

[6] H. Poulos, H. Chow, and J. Small, (2019) *"The use of equivalent circular piles to model the behaviour of rectangular barrette foundations"* **Geotechnical Engineering Journal of the SEAGE and AGSSEA *50***(3): 106–109.

[7] G. Plumbridge, J. Sze, and T. Tham. "Full-scale lateral load tests on bored piles and a barrette". In: *Proceedings of the Nineteenth Annual Seminar*. 2000, 211–220.

[8] C. W. Ng, D. B. Rigby, S. W. Ng, and G. Lei, (2000) *"Field studies of well-instrumented barrette in Hong Kong"* **Journal of geotechnical and geoenvironmental engineering *126***(1): 60–73.

[9] C. W. Ng and G. Lei, (2003) *"Performance of long rectangular barrettes in granitic saprolites"* **Journal of geotechnical and geoenvironmental engineering *129***(8): 685–696. DOI: 10.1061/(ASCE)1090-0241(2003)129:8(685).

[10] G. Lei, X. Hong, and J. Shi, (2007) *"Approximate three-dimensional analysis of rectangular barrette–soil–cap interaction"* **Canadian geotechnical journal *44***(7): 781–796. DOI: 10.1139/t07-017.

[11] S.-S. Lin, F.-C. Lu, C.-J. Kuo, T.-W. Su, and E. Mulowayi, (2014) *"Axial capacity of barrette piles embedded in gravel layer"* **Journal of GeoEngineering *9***(3): 103–107. DOI: 10.6310/jog.2014.9(3).3.

[12] M. Hsu. *"The bearing behavior of barrette piles under vertical loading", Doctoral Dissertation"*. (in china). (phdthesis). National Taiwan University, 2017.

[13] G. Kacprzak and S. Bodus, (2018) *"Analysis of the barrette load investigation of the tallest building in European Union"* **Archives of Civil Engineering**: 281–292. DOI: 10.2478/ace-2018-0057.

[14] S. Rafa and B. Moussai, (2018) *"Three-dimensional analyses of bored pile and barrette load tests subjected to vertical loadings"* **Soil Mechanics and Foundation Engineering *55***(3): 146–152.

[15] D. Chang, C. Lin, T. Wang, Y. Lin, F. Lu, and C. Kuo, *"Three-dimensional Finite Element Analyses of Barrette Piles under Compression and Uplift Loads with Field Data Assessments"*:

[16] L. Zhang, (2003) *"Behavior of laterally loaded large-section barrettes"* **Journal of Geotechnical and Geoenvironmental Engineering *129***(7): 639–648. DOI: 10.1061/(ASCE)1090-0241(2003)129:7(639).

[17] A. El Wakil and A. K. Nazir, (2013) *"Behavior of laterally loaded small scale barrettes in sand"* **Ain Shams Engineering Journal *4***(3): 343–350. DOI: 10.1016/j.asej.2012.10.011.

[18] E. Conte, A. Troncone, and M. Vena, (2013) *"Nonlinear three-dimensional analysis of reinforced concrete piles subjected to horizontal loading"* **Computers and Geotechnics *49***: 123–133. DOI: 10.1016/j.compgeo.2012.10.013.

[19] D. Bahloul and B. Moussai. "Three-dimensional analysis of laterally loaded barrette foundation using Plaxis 3D". In: *Civil Engineering Conf. in The Asian Region*. 2016.

[20] A. J. Wang S.T and V. L.G. *APILE 2018- User's Manual*. 2018.

[21] Midas. *Midas GTS NX User Manual*. 2014.

[22] C. Lin. *"Numerical analysis on barrette pile bearing mechanism under vertical loading"*. in Chinese. (mathesis). Dept. of Civil Engineering, Tamkang University, 2018.

[23] Y. Tsai. *"Case study for axial load test of wall-type piles", Master Thesis, Dept. of Civil Engineering"*. in Chinese. (mathesis). National Taiwan University, 2006.

[24] Construction and C. Planning Agency. *Seismic Design Code for Buildings*. MOI, Taiwan. 2011.

[25] S. E. Dickenson. *"Dynamic response of soft and deep cohesive soils during the Loma Prieta earthquake of October 17, 1989"*. (phdthesis). University of California, Berkeley, 1994.

[26] S. A. Ashford, W. Jakrapiyanun, and P. Lukkunaprasit. "Amplification of earthquake ground motions in Bangkok". In: *Proceedings of the 12th World Conference on Earthquake Engineering, Auckland, New Zealand*. 2000, 1–7.

[27] M. Hatanaka and A. Uchida, (1996) *"Empirical correlation between penetration resistance and internal friction angle of sandy soils"* **Soils and foundations *36***(4): 1–9. DOI: 10.3208/sandf.36.4_1.

[28] M. Davisson and H. Gill, (1963) *"Laterally loaded piles in a layered soil system"* **Journal of the Soil Mechanics and Foundations Division *89***(3): 63–94. DOI: 10.1061/JSFEAQ.0000521.

[29] H. Matlock and L. C. Reese, (1960) *"Generalized solutions for laterally loaded piles"* **Journal of the Soil Mechanics and foundations Division *86***(5): 63–92. DOI: 10.1061/JSFEAQ.0000303.

[30] A. Keceli, (2012) *"Soil parameters which can be determined with seismic velocities"* **Jeofizik *16***(1): 17–29.

[31] Y. Chang. "Discussion on Lateral Pile-Loading Tests by Feagin". In: *ASCE*. 1937, 272–278.